

Document downloaded from:

<http://hdl.handle.net/10251/71420>

This paper must be cited as:

De Rosa, M.; Ruiz Calvo, F.; Corberán Salvador, JM.; Montagud Montalvá, CI.; Tagliafico, L. (2015). A novel TRNSYS type for short-term borehole heat exchanger simulation: B2G model. *Energy Conversion and Management*. 100:347-357.
doi:10.1016/j.enconman.2015.05.021



The final publication is available at

<http://dx.doi.org/10.1016/j.enconman.2015.05.021>

Copyright Elsevier

Additional Information

“A novel TRNSYS type for short-term borehole heat exchanger simulation: B2G model”

by

Mattia De Rosa^{*a}, Félix Ruiz Calvo^b, José M. Corberán^b, Carla Montagud^b,
Luca A. Tagliafico^a

^a *DIME/TEC – Division of Thermal Energy and Environmental Conditioning, University of Genoa, via All’Opera Pia 15/A 16145, Genoa, Italy.*

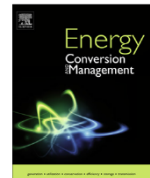
^b *Instituto de Ingeniería Energética, Universitat Politècnica de València. Camino de Vera sn 46022 Valencia, Spain.*



Contents lists available at [ScienceDirect](#)

Energy Conversion and Management

journal homepage: www.elsevier.com/locate/enconman



To be published in Energy Conversion and Management

DOI: [10.1016/j.enconman.2015.05.021](https://doi.org/10.1016/j.enconman.2015.05.021)

Highlights

A novel dynamic Borehole Heat Exchanger model is presented.

Theoretical approach for model parameters calculation is described.

The short-term model is validated against experimental data of a real GSHP.

Strong dynamic conditions due to the ON-OFF regulation are investigated.

(*) corresponding author – Dr. Mattia De Rosa
email: mattia.derosa@unige.it; m_derosa@hotmail.it

A novel TRNSYS type for short-term borehole heat exchanger simulation: B2G model

Mattia De Rosa^{a,*}, Félix Ruiz-Calvo^b, José M. Corberán^b, Carla Montagud^b, Luca A. Tagliafico^a

^a*DIME/TEC - Division of Thermal Energy and Environmental Conditioning, University of Genova. Via dell'Opera Pia 16145 Genova, Italy. Phone: +39-010-3532578. Fax: +39-010-311870*

^b*Instituto de Ingeniería Energética, Universitat Politècnica de València. Camino de Vera sn 46022 Valencia, Spain. Phone: +34-96-3879910. Fax: +34-963877272*

Abstract

Models of ground source heat pump (GSHP) systems are used as an aid for the correct design and optimization of the system. For this purpose, it is necessary to develop models which correctly reproduce the dynamic thermal behavior of each component in a short-term basis. Since the borehole heat exchanger (BHE) is one of the main components, special attention should be paid to ensuring a good accuracy on the prediction of the short-term response of the boreholes. The BHE models found in literature which are suitable for short-term simulations usually present high computational costs. In this work, a novel TRNSYS type implementing a borehole-to-ground (B2G) model, developed for modeling the short-term dynamic performance of a BHE with low computational cost, is presented. The model has been validated against experimental data from a GSHP system located at Universitat Politècnica de València, Spain. Validation results show the ability of the model to reproduce the short-term behavior of the borehole, both for a step-test and under normal operating conditions.

Keywords: ground source heat pump, borehole heat exchanger, heating and cooling systems, dynamic modeling

*Corresponding author at: DIME/TEC - Division of Thermal Energy and Environmental Conditioning, University of Genova. Via dell'Opera Pia 16145 Genova, Italy.

Email addresses: mattia.derosa@unige.it; m_derosa@hotmail.it (Mattia De Rosa), fliruica@etsii.upv.es (Félix Ruiz-Calvo), corberan@upvnet.upv.es (José M. Corberán), carmonmo@iie.upv.es (Carla Montagud), tgl@ditec.unige.it (Luca A. Tagliafico)

Preprint submitted to Energy Conversion and Management

April 18, 2015

1 **1. Introduction**

2 Geothermal energy systems have been recognized as being among the
3 most efficient and comfortable heating and cooling systems currently avail-
4 able by the U.S. Environmental Protection Agency [1], presenting several
5 advantages respect to air source heat pumps [2]. Ground source heat pumps
6 (GSHP) represent one of the common available and profitable geothermal
7 systems, using the ground as a heat source in winter and as a heat sink in
8 summer. Generally, the heat exchange takes place in a ground source heat
9 exchanger (GSHE) and different configurations can be adopted. Among
10 those, one of the most commonly used is the vertical borehole field, consist-
11 ing on a certain number of boreholes drilled in the ground, inside which the
12 heat carrier fluid exchanges heat with the surrounding ground, depending
13 on the operating conditions.

14 Ever since the first GSHPs were installed, lots of research works have
15 been addressed to the analysis and modeling of this kind of installations. Re-
16 cent works are performed in order to investigate the thermodynamic aspects
17 [3, 4], the geometries and the system thermal performance [5, 6, 7, 8, 9],
18 and involving numerical issues [10, 11, 12]. An interesting overall review on
19 these systems with a comparison with other technologies can be found in
20 [13].

21 In this context, obtaining an accurate model for the GSHE has been
22 one of the main focuses of research through the last years, in which several
23 approaches with different characteristics have been considered (an accurate
24 review on the different models is presented by Yang et al. [14]). Some of
25 them are discussed in the following, focusing on one of the most common
26 borehole configurations: vertical boreholes with U tubes.

27 Eskilson [15] proposed a steady state model combining analytical and
28 numerical solution techniques. It is based on the use of non-dimensional
29 temperature response factors, called g-functions, that represent the tem-
30 perature response to a constant heat injection pulse, for a certain time step.
31 Then, the actual thermal load is divided into a series of step loads and the
32 temperature response of the borehole is obtained by superimposing the sin-
33 gle response at each step. Another version of this approach consists in using
34 an exponential integral function, as presented in [16]. Eskilson obtained the
35 g-function through a two-dimensional numerical calculation: with this ap-
36 proach, it is possible to calculate the borehole temperature in time steps
37 greater than $5r_b/\alpha$, which results in 3 to 6 hours for a typical borehole. In
38 [17], the g-functions calculated by Eskilson are extended to shorter time
39 steps. After calculating the borehole temperature, it is possible to obtain
40 the outlet fluid temperature by means of the borehole resistance and of the
41 entering fluid temperature. The g-function is widely used in simulation and
42 design software, such as GLHEPRO [18] or EED [19], and it has been im-
43 proved in the last years, for example, generating numerically g-functions for
44 specific GSHE geometries, as in [20]. The temporal superposition method
45 is also at the base of the BHE design procedure presented by Deerman and
46 Kavanaugh [21] and later refined by Kavanaugh and Rafferty [22] which is
47 adopted as standard in the Ashrae Handbook [23]. A useful description of
48 this model and a recent calculation procedure to calculate proper response
49 factor are presented in [24]. Recently, Koochi-Fayegh and Rosen [25] pro-
50 posed a semi-analytical approach to couple a model outside the borehole,
51 based on the transient finite line-source model, with one inside the borehole
52 which assumes a steady-state heat conduction.

53 Another approach to numerically describe a vertical borehole is the ther-
54 mal network model, in which the borehole and the surrounding ground are
55 represented as a series of temperature nodes connected by thermal resis-
56 tances. In order to model the thermal inertia, thermal capacitances are
57 added to the temperature nodes [26]. The basic thermal network is the
58 delta network, with one node on each pipe of the U tube and one node at
59 the borehole wall [27] (Figure 1). Many improvements have been made to
60 the delta network, usually adding more nodes to the network, as in [28, 29]
61 and [30], or dividing the borehole into two or more areas, depending on
62 the internal borehole geometries [31]. The thermal network approach can
63 also be used for modelling the behavior of the ground around the borehole,
64 from the undisturbed ground temperature to the borehole wall. However,
65 if a high accuracy is desired, the network has to be very fine, increasing the
66 number of temperature nodes, which results in a greater number of differen-
67 tial equations that must be solved causing a longer simulation time needed.
68 The borehole thermal resistance is used in the thermal network approach,
69 since it represents the resistance between the pipes and the borehole wall.
70 This resistance can be experimentally obtained, as described in [31], or it
71 can be calculated analytically. Furthermore, Lamarche et al. [31] present
72 an exhaustive review of different methods to obtain the borehole resistance
73 starting from the borehole geometry and from the thermal characteristics of
74 fluid, pipes and grout. In Sharqawy et al. [32], a correlation for the borehole
75 resistance is obtained numerically and compared with approximate analyt-
76 ical solutions.

77 Finally, the finite elements model (FEM) represents one of the more
78 detailed models available in literature (some examples can be found in [33,

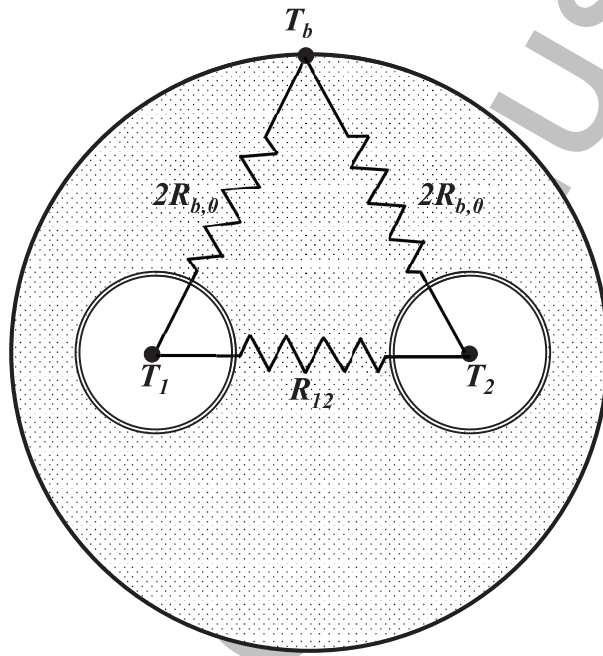


Figure 1: Standard steady state delta network [27].

79 34], [35], and [36]), which allows to obtain the most accurate results despite
80 a high computational cost, due to the more detailed discretization of the
81 borehole and of the surrounding ground. Therefore, FEM models are usually
82 assumed as a reference for validation of simpler models that can provide
83 faster simulation results, although not being so accurate.

84 Several other numerical models have been developed in the last years (as,
85 e.g., [37, 38]) adopting different approaches (see [39, 40]). Most of them can
86 only be used to simulate the borehole thermal performance for long time
87 steps, usually greater than an hour without reproducing the short-term
88 dynamic behavior. However, the dynamic short-term behavior becomes a
89 relevant issue, especially considering that GSHEs are generally integrated in
90 other complex systems, in which the short-term regulation criteria assume
91 an important role in the energy performance of the whole system. For these
92 reasons, steady state models or dynamic models with higher timescale are
93 not useful for analyzing and optimizing these complex systems. In this
94 context, more complex models, such as FEM, in which a detailed description
95 of the heat transfer phenomenon inside the borehole is provided are not
96 convenient due to their high computational costs.

97 A complete model of a GSHP system for heating and cooling in an of-
98 fice building located at the Universitat Politècnica de València (UPVLC),
99 in Spain, has recently been developed by the authors [41], using TRNSYS
100 simulation software [42]. The system operation is based on an ON/OFF
101 control, commonly used in this kind of installations. The characteristic wa-
102 ter temperature evolution due to the ON/OFF cycling of the heat pump
103 has a great influence in the design and optimization of the installation. In
104 this context, due to the low characteristic time (minutes) for the different

105 system components (tank, pipes, heat pump, etc.), it is necessary to find a
106 GSHE model that is able to reproduce the thermal behavior of the boreholes
107 for very short heat injection/extraction periods. Furthermore, since it is to
108 be embedded in a global complex model developed in the TRNSYS envi-
109 ronment, a low computational time becomes key for modeling the GSHE.
110 Therefore, FEMs cannot be used for the purpose of this work. On the other
111 hand, steady state models are neither appropriate for this aim, since they
112 are not meant to predict short-term behavior.

113 At the UPVLC GSHP installation, the duration of the ON periods of the
114 heat pump is about 10 minutes, although it depends on the thermal load and
115 the implemented control algorithm. The system is switched on normally 15
116 hours a day, but the total heat injection/extraction period may vary from
117 1.5 to 10 hours, depending on the thermal load for each day. Due to this
118 particular operation, in the GSHE, the system thermal load may only affect
119 a reduced volume around the boreholes, in the short-term. Therefore, the
120 thermal response of a borehole for an operational day can be modeled just
121 taking into account the ground near the borehole. The novelty of the ap-
122 proach proposed in this paper consists in using two separate models for the
123 local and global solution calculation. Thus, the short-term and long-term
124 simulation are decoupled and faster models can be used on each side. On
125 one hand, the short-term model only takes into account the ground volume
126 directly affected by the heat injection/extraction period of an operational
127 day. This model should be able to reproduce the instantaneous response
128 of the BHE due to the ON-OFF operation, for a total operating time of
129 15 hours. For this purpose, the model uses the initial ground temperature
130 of each day as a starting point of the calculations. Therefore, a long-term

131 model able to calculate the initial ground temperature for each day, taking
132 into account the thermal load of the previous one, is required. The total
133 computational cost of the global model resulting from the combination of
134 both short and long-term models is reduced, since the long-term response
135 of the ground is calculated on a daily basis, instead of being calculated at
136 every time-step.

137 The aim of the present work is to present a new TRNSYS type spe-
138 cially developed for modelling the short-term behavior of a borehole heat
139 exchanger (BHE). The TRNSYS type implements a novel dynamic model,
140 called borehole-to-ground (B2G) model, which is able to simulate the short-
141 term behavior of a single U-tube borehole over a period of at least 10-15
142 hours. This short-term model can be coupled with a standard steady-state
143 long-term model, such as the g-function, in order to take into account the
144 long-term behavior of the ground, e.g. correcting the initial ground tem-
145 perature for each simulated day. B2G model was initially presented in [11],
146 where it was validated against experimental data from a BHE located in
147 Stockholm, Sweden. Moreover, a comparison of the performance of B2G
148 with that of a standard steady-state model can be found in [43]. In particu-
149 lar, B2G model was compared to the one already programmed in the TRN-
150 SYS software (type 557), which implements the Duct Ground Heat Storage
151 Model (DST) developed by Hellström [44]. As reported in [43], DST model
152 is a useful model able to produce a good estimation of the ground temper-
153 ature at the boreholes along the years. Nevertheless, its main limitation is
154 the steady-state assumption and the neglect of the advection effect in the
155 outlet water temperature calculation procedure, which could affect strongly
156 the performance of the model for very short time steps like the ones existing

157 in ON/OFF GSHP systems.

158 The aim of the present paper is to extend the validation of B2G model to
159 stronger dynamic conditions which occur typically with ON/OFF regulation
160 criteria. A detailed description of the model equations and procedures is
161 reported in 2.1. The validation is performed comparing the numerical results
162 provided by B2G against experimental measurements from GeoCool plant,
163 installed at Universitat Politècnica de València [45], which operates under
164 an ON/OFF control algorithm, as described in section 3.1. In particular,
165 B2G model is validated considering two different operating conditions: (i)
166 a step-test in cooling mode and (ii) during standard operating mode in two
167 different typical days, one for heating mode and one for cooling mode.

168 **2. B2G model**

169 *2.1. B2G model description*

170 Starting from previous works [28, 29, 30, 31, 38], B2G dynamic numerical
171 model was developed and tested in order to reproduce the behavior of a
172 single U-tube in a short-term scale. B2G model was first presented in Ruiz-
173 Calvo et al. [11]. As stated in section 1, the model is focused on the
174 short-term behavior prediction. Therefore, it takes into account only the
175 BHE itself and the portion of its surrounding ground that is directly affected
176 during the heat injection period considered. A detailed description of the
177 B2G model is provided below, while a schematic figure of the calculation
178 procedure is shown in Figure 2.

179 B2G model is based on a 2D thermal network model coupled with a ver-
180 tical discretization of the entire domain (Figure 3b): at each z-depth, the
181 two-dimensional thermal network (Figure 3a) describes the heat transfer

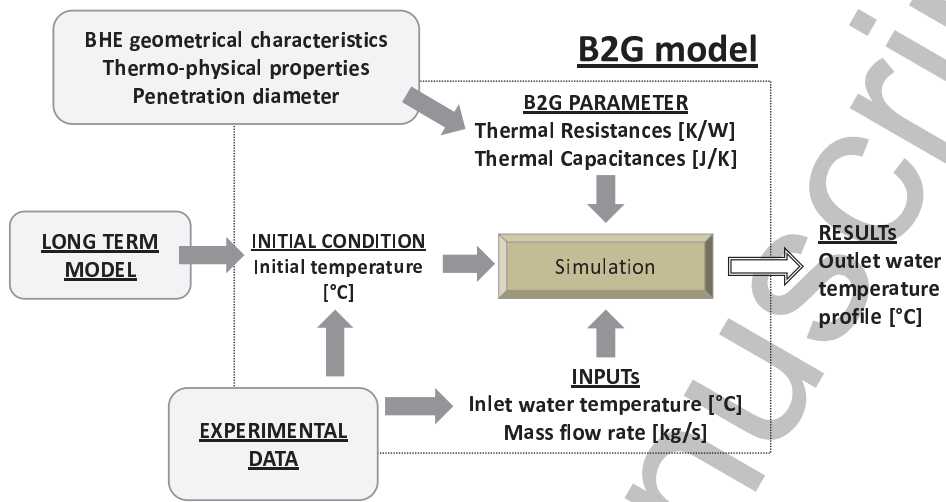


Figure 2: Calculation procedure of B2G model

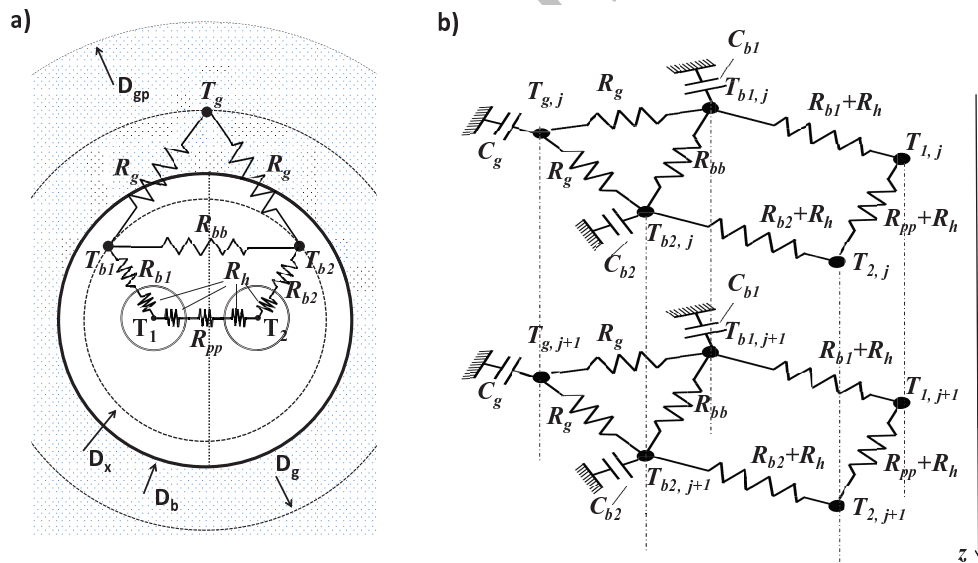


Figure 3: Thermal network model adopted in the present work: a) 2D model; b) 3D model.

182 between temperature nodes, in which thermal capacitances are lumped, by
 183 using thermal resistances. The grout inside the borehole is modeled consid-
 184 ering two different regions, as shown in Figure 3a, resulting in two different
 185 borehole nodes [31] with a lumped thermal capacitance (the position of
 186 these nodes is discussed in section 2.2). Neglecting vertical conduction,
 187 the energy balance equations corresponding to the different nodes of the
 188 thermal network correspond to Eqs. 1 to 5.

$$\frac{\partial T_1(z)}{\partial t} = -v \frac{\partial T_1(z)}{\partial z} - \frac{1}{c_f} \left(\frac{T_1(z) - T_{b1}(z)}{R_{b1}} + \frac{T_1(z) - T_2(z)}{R_{pp}} \right) \quad (1)$$

$$\frac{\partial T_2(z)}{\partial t} = -v \frac{\partial T_2(z)}{\partial z} - \frac{1}{c_f} \left(\frac{T_2(z) - T_{b2}(z)}{R_{b2}} - \frac{T_1(z) - T_2(z)}{R_{pp}} \right) \quad (2)$$

$$c_{b1} \frac{\partial T_{b1}(z)}{\partial t} = \frac{T_1(z) - T_{b1}(z)}{R_{b1}} + \frac{T_{b1}(z) - T_{b2}(z)}{R_{bb}} - \frac{T_{b1}(z) - T_g(z)}{R_g} \quad (3)$$

$$c_{b2} \frac{\partial T_{b2}(z)}{\partial t} = \frac{T_2(z) - T_{b2}(z)}{R_{b1}} - \frac{T_{b1}(z) - T_{b2}(z)}{R_{bb}} - \frac{T_{b2}(z) - T_g(z)}{R_g} \quad (4)$$

$$c_g \frac{\partial T_g(z)}{\partial t} = \frac{T_{b1}(z) - T_g(z)}{R_g} + \frac{T_{b2}(z) - T_g(z)}{R_g} \quad (5)$$

191 For the fluid nodes, the advection in vertical direction has been taken
 192 into account in the transient energy balance equation (Eqs. 1 and 2).

193 The entire model consists of a system of ordinary differential equations,
 194 with five thermal capacitances and six thermal resistances at each z-depth
 195 (5C6R-n model, where n is the number of the nodes), which can be solved
 196 using standard numerical procedures as described in [11]. The thermal
 197 network configuration considered for the B2G model has been chosen in

198 order to accomplish the two main aims of the model: reducing the number
199 of parameters as much as possible while ensuring a good accuracy of the
200 model for short-time response prediction.

201 2.2. Parameter calculation

202 For a given borehole, where the geometrical characteristics and thermo-
203 physical properties are known, it is possible to determine the borehole ca-
204 pacitances and resistances for the model. This section presents the final
205 equations that allow to calculate the parameters of the B2G model, as pre-
206 sented in [11].

207 2.2.1. Grout nodes

208 Considering each grout zone, the thermal capacitances C_{b1} and C_{b2} can
209 be calculated as follows:

$$C_{b1} = C_{b2} = dz \cdot \left(\frac{S_b}{2} c_b + S_p c_p \right) \approx dz \cdot \frac{S_b}{2} c_b \quad (6)$$

210

$$S_b = \frac{\pi}{4} (D_b^2 - 2D_{p,e}^2) \quad (7)$$

211 where S_b is the borehole section neglecting the pipes, dz is the node length
212 and c_b is the grout volumetric heat capacity. Since the thermal capacitance
213 of the pipe walls is small, compared to that of the grout, the term $S_p c_p$ is
214 neglected in equation 6.

215 Figure 4 shows the different steps that have been carried out for the
216 thermal resistances determination.

217 The thermal resistances between the grout and pipe nodes depend on the
218 overall borehole thermal resistance R_{BHE} (Figure 4a), usually determined
219 by experimental tests. Generally, it is possible to divide the global borehole

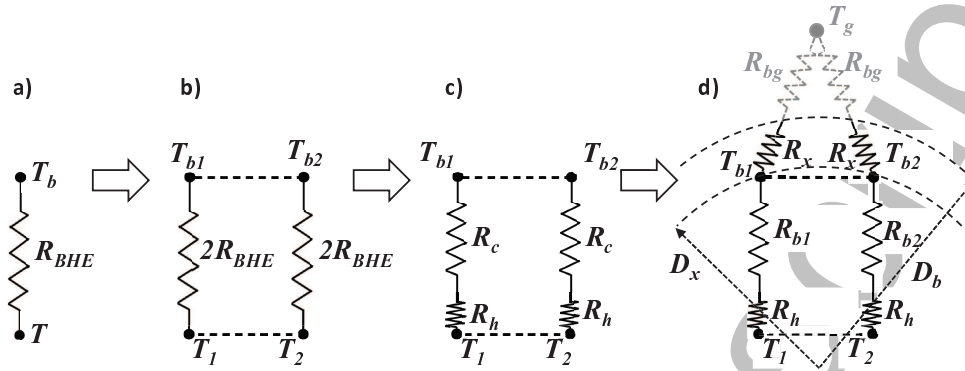


Figure 4: Thermal resistances definition steps: a) borehole resistance, b) parallel borehole resistances, c) convective and conductive resistances, d) final resistances configuration.

220 thermal resistance R_{BHE} into two thermal parallel resistances connecting
 221 each pipe with the corresponding grout zone (Figure 4b). Moreover a con-
 222 vective (R_h) and a conduction term (R_c) can be identified (Figure 4c) and
 223 the relationship shown in Eq. 8 can be written.

$$2R_{BHE} = R_h + R_c \quad (8)$$

224 Since the grout nodes are located somewhere in between the pipes and
 225 the borehole wall, at a certain diameter D_x , the conductive thermal resis-
 226 tance on equation 8, R_c , is divided into two different resistances (Figure
 227 4d), following Eq. 9.

$$R_c = R_b + R_x \quad (9)$$

where $R_b = R_{b1} = R_{b2}$

228 The parameters R_{b1} and R_{b2} from the thermal network (Figure 3) cor-
 229 respond to the parameter R_b on Eq. 9. On the other hand, the thermal
 230 resistance R_g of the B2G model is determined adding the resistance between

231 the grout nodes and the borehole wall R_x to the ground thermal resistance
 232 R_{bg} (Figure 4d), as shown in Eq. 10.

$$R_g = R_{bg} + R_x \quad (10)$$

233 The mean convection term R_h is calculated assuming a mean value of
 234 the convective heat transfer coefficient (h) inside the pipes (Eq. 11):

$$R_h = \frac{1}{\pi D_{p,i} dz h} = \frac{1}{\pi dz Nu k} \quad (11)$$

235 where (Nu) is the Nusselt number which can be calculated according to the
 236 appropriate correlation depending on the flow regime (e.g. [46]), and $D_{p,i}$
 237 is the internal pipe diameter.

238 For the calculation of the conduction thermal resistance, an equivalent
 239 surface has been determined, which represents the pipes surface and allows
 240 to solve the heat transfer problem as a semi-cylindrical conductive heat
 241 transfer (Figure 5a). For the equivalent surface, the approach suggested by
 242 Pasquier et al. [30] has been used, giving the equivalent diameter shown in
 243 Eq. 12.

$$D_{eq} = D_{p,e} \sqrt{\frac{4W}{\pi D_{p,e}} + 1} \quad (12)$$

244 Thus, the conduction thermal resistance for each borehole zone is calcu-
 245 lated considering the conductive heat transfer in a semi-cylinder (Eqs. 13,
 246 14):

$$R_b = \frac{\ln(D_x/D_{eq})}{\pi k_b dz} \quad (13)$$

$$R_x = \frac{\ln(D_b/D_x)}{\pi k_b dz} \quad (14)$$

248 where D_x is the position of the borehole nodes, with $D_{eq} < D_x < D_b$ (Figure
249 5b).

250 As reported in Lamarche et al. [31], the position D_x depends strictly
251 on the internal borehole geometry, especially on the shank spacing and it
252 is not possible to determine it *a priori*. Generally, if the shank spacing
253 is high and, therefore, the pipes are quite close to the borehole wall, it is
254 advisable to locate the nodes directly on the borehole diameter ($D_x = D_b$).
255 Otherwise, an approximation could be obtained by means of a sensitivity
256 analysis on the effect of different D_x comparing the numerical results with
257 the experimental ones obtained in a step-test.

258 The thermal resistance between the pipe nodes (R_{pp}) is quite complex
259 to obtain due to the two-dimensional heat transfer phenomena occurring in
260 this grouting zone. In order to simplify the calculation, the maximum value
261 is assumed as a limit, considering a one-dimensional linear heat conduction
262 between them (Figure 5c). Analogue to this, a one-dimensional heat transfer
263 between the two borehole nodes is assumed (R_{bb}) through the remaining
264 surface, as shown in Figure 5d:

$$R_{pp} = \frac{W - D_{p,e}}{D_{p,e} dz k_b} \quad (15)$$

$$R_{bb} = \frac{W}{k_b (D_b - D_{p,e}) dz} \quad (16)$$

266 2.2.2. Ground node

267 The thermal capacitance of the ground, C_g , depends essentially on the
268 penetration depth, D_{gp} , of the borehole. The penetration depth depends
269 on the heat injection/extraction time and on the ground thermal properties
270 and. In the B2G model, it becomes an adjusting parameter which depends

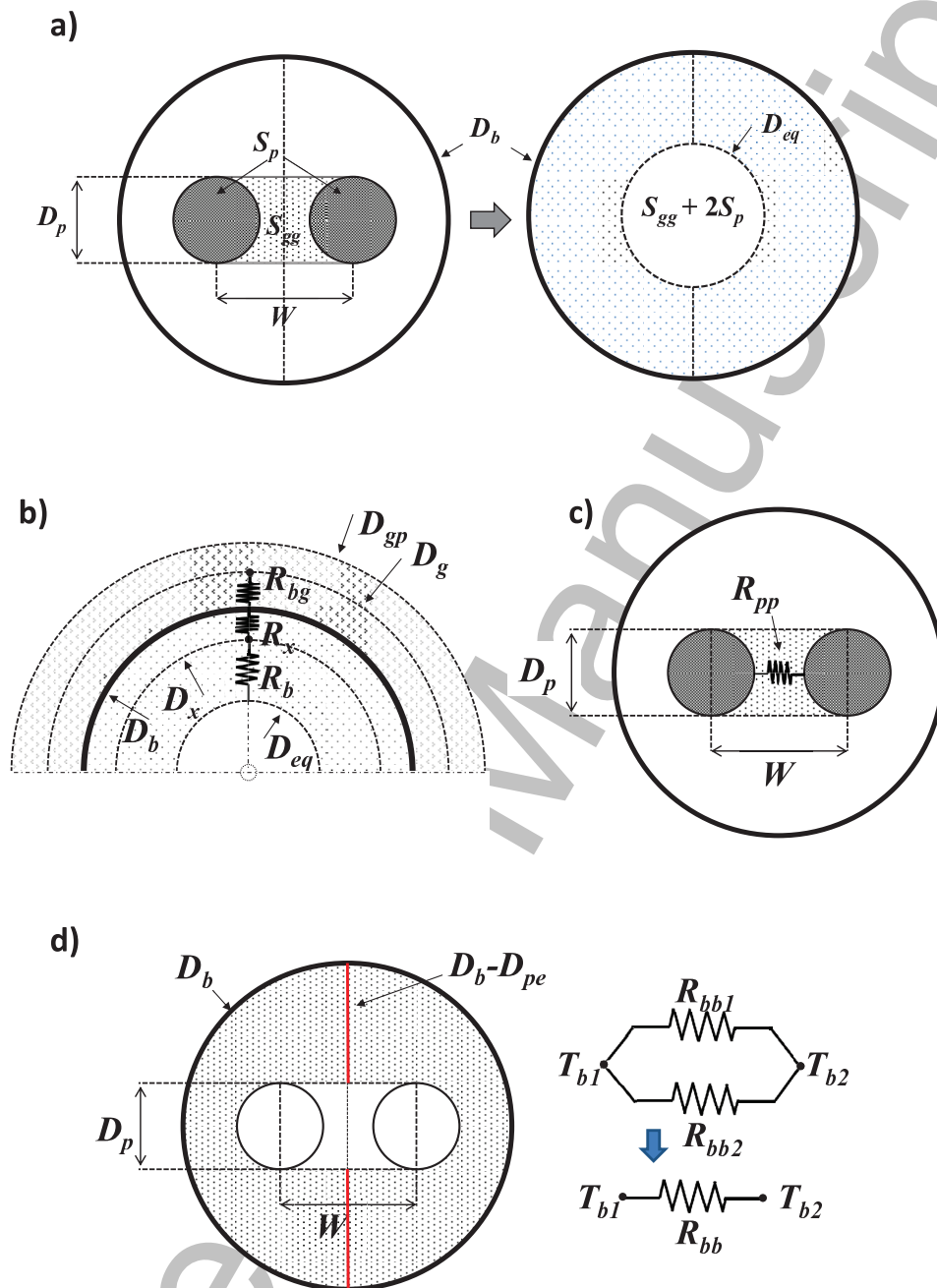


Figure 5: Geometrical model characteristics to calculate a) the equivalent diameter [30], b) borehole node position, c) pipe to pipe thermal resistance, d) borehole node to borehole node thermal resistance.

271 on the simulation time considered. For a given penetration depth, it is
272 possible to calculate directly the thermal capacitance, C_g , as follows:

$$C_g = \frac{\pi}{4} (D_{gp}^2 - D_b^2) c_g dz \quad (17)$$

273 On the other hand, assuming that all the ground thermal capacitance is
274 lumped in the diameter D_g , calculated as the average between the borehole
275 diameter, D_b , and the penetration diameter, D_{gp} , the corresponding thermal
276 resistance of the ground R_{bg} is calculated with Equation 18.

$$R_{bg} = \frac{1}{\pi k_g dz} \ln \left(\frac{D_g}{D_b} \right) \quad (18)$$

277 Finally, the thermal resistance R_g in Eq. 3-5 can be calculated by means
278 of Equation 19.

$$R_g = R_x + R_{bg} \quad (19)$$

279 3. Model validation

280 3.1. GeoCool Plant

281 GeoCool plant is a demonstration facility located at the Universitat
282 Politècnica de València (UPVLC), Spain. It was built in the framework of
283 a FP5 European project named 'GeoCool' project [45]. The system consists
284 of a reversible ground source heat pump (GSHP) that provides the air con-
285 ditioning for a set of spaces in the Department of Applied Thermodynamics
286 at UPVLC (Figure 6). The heating nominal capacity of the heat pump is
287 17kW (with water return temperatures of 35°C and 17°C) and the cooling
288 nominal capacity is 14.7kW (with water return temperatures of 14°C and
289 25°C). The total air conditioned area is approximately 250m².

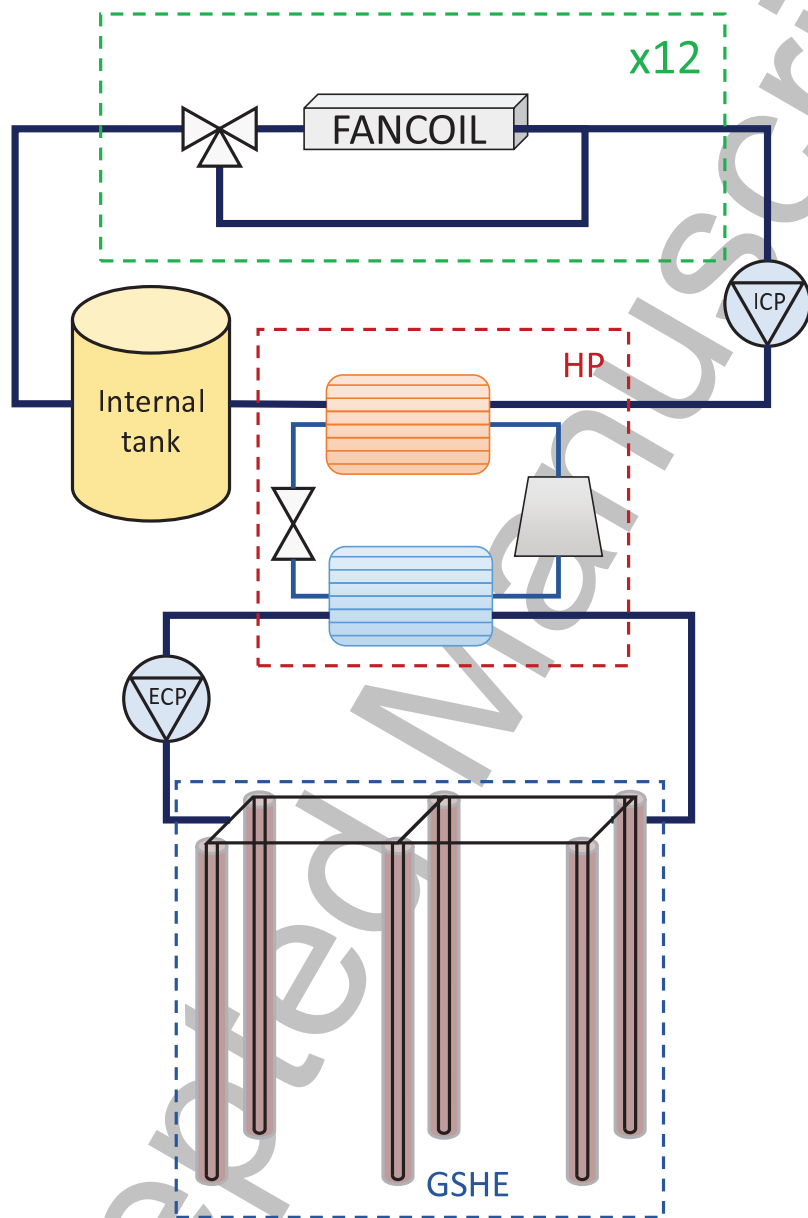


Figure 6: GeoCool schematic diagram with the internal and external circuits.

290 A detailed description of the installation and the particular conditions of
291 its operation is provided in [8]. In [47], the design and construction process
292 of the installation was presented, including the design of the ground source
293 heat exchanger (GSHE). Figure 6 shows the basic scheme of the installation.
294 The reversible GSHP is connected to an external circuit and an internal
295 circuit. The internal circuit includes a total of 12 parallel connected fan-
296 coils, an hydraulic loop for water distribution, a water storage tank and a
297 circulation pump. On the other hand, the external circuit comprises the
298 GSHE, a circulation pump, and the corresponding hydraulic loop.

299 The system has been working since February 2005, and it has been
300 completely monitored during all its operation time. The installation is
301 programmed to work 15 hours a day, five days per week, being switched off
302 during the nights and the weekends. During its normal operation, the heat
303 pump controller switches on/off the compressor depending on the controlled
304 temperature. The external circulation pump switches on/off together with
305 the heat pump, with a lag of one minute: it switches on one minute before
306 the heat pump, and switches off one minute later. The internal circulation
307 pump is continuously switched on during the 15 hours of operation of the
308 system. A detailed description of the GSHE is provided in the section 3.1.1.

309 The on/off cycling of the heat pump and the external circulation pump
310 results in a characteristic temperature evolution along the day. Figure 7
311 shows the evolution of the water temperatures entering and exiting the heat
312 pump, for a typical heating and cooling day. The on/off cycles of the heat
313 pump are reflected in the water temperatures, both in the internal and the
314 external circuit, which periodically increase and decrease. Typical water
315 temperatures entering the boreholes are around 30°C in cooling periods

316 and 14°C in heating periods, while the exiting water temperatures from the
317 BHE range from 25°C to 17°C, respectively. A more detailed analysis of
318 the water temperatures of the system and their evolution along the years
319 can be found in [48].

320 The system performance has been monitored by a network of sensors
321 that measures the temperature, mass flow, and power consumption. The
322 temperature sensors are four-wire PT100 with accuracy ± 0.1 C. The mass
323 flow meters are Danfoss Coriolis meters, model massflo MASS 6000 with
324 signal converter Compact IP 67 and accuracy < 0.1 %. The power meters
325 are multifunctional power meters from Gossen Metrawatt, model A2000
326 with accuracy ± 0.5 % of the nominal value. Reference data sets obtained
327 from the installation were published in [8].

328 *3.1.1. Ground Source Heat Exchanger*

329 The GSHE was designed according to the building demand, in order to
330 minimize the impact of the installation on the ground thermal response.
331 An analysis of the impact of the installation after the first five years of
332 operation is presented in [48]. The analysis confirms the correct design of
333 the installation, since the water return temperatures from the GSHE are
334 nearly constant for each year.

335 The GSHE consists of 6 vertical boreholes, connected in parallel, and
336 arranged in a 2 x 3 rectangular grid, with a 3 m spacing between boreholes.
337 Each borehole has a nominal diameter of 150 mm and it is 50 m deep
338 containing a single HDPE U-tube. The inner and external diameters of
339 the U-tube are 25.4 mm and 32 mm respectively, with a center-to-center
340 distance (shank spacing) of 70 mm. All boreholes are filled with sand and

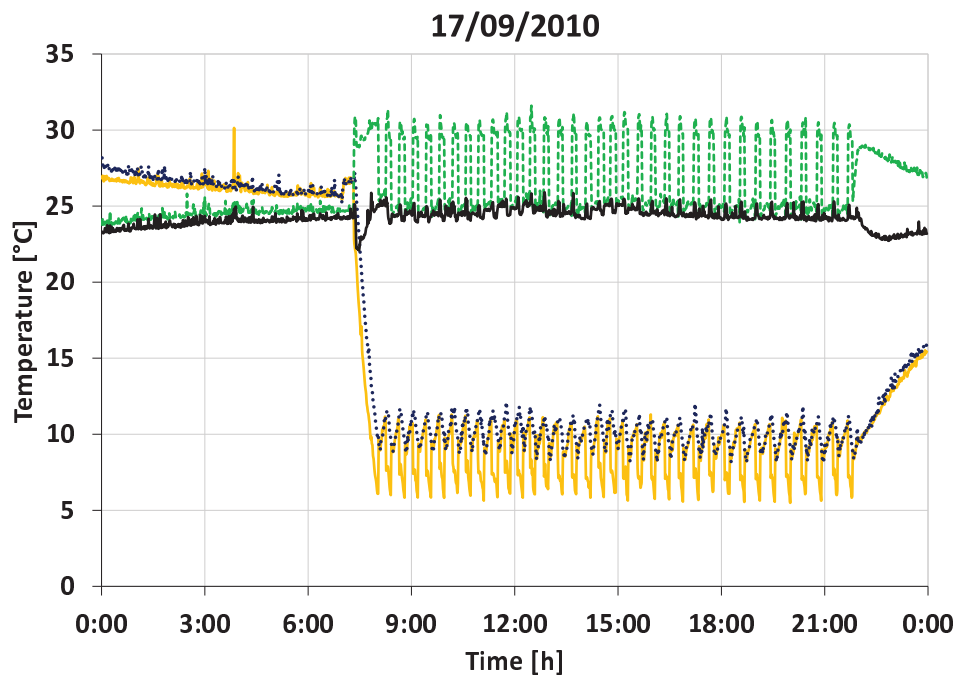
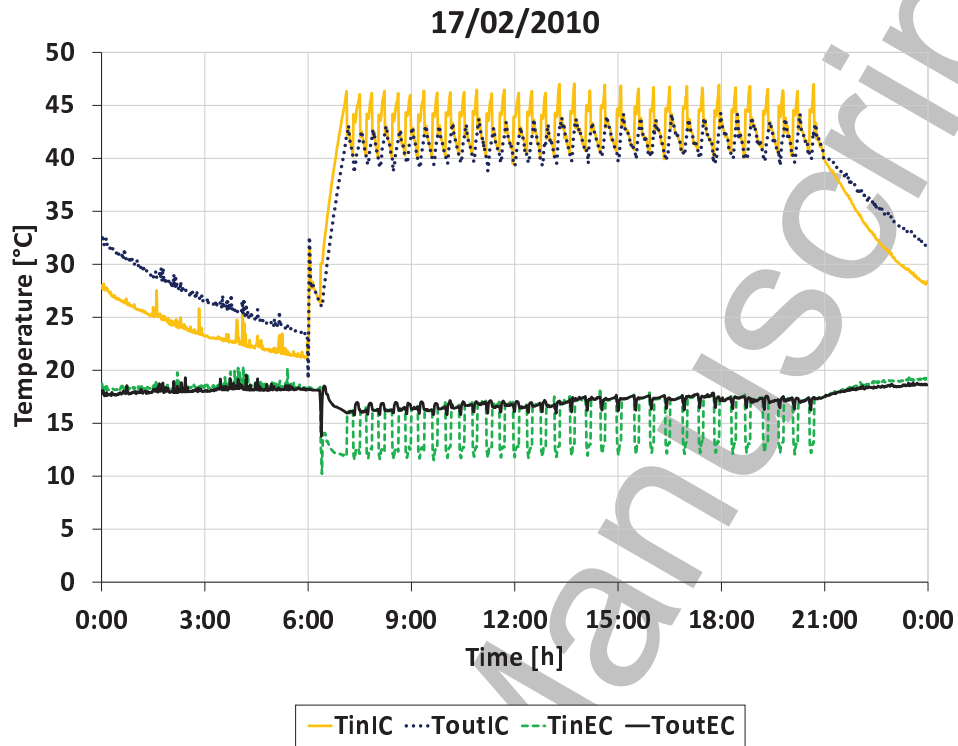


Figure 7: Evolution of the water temperatures at the internal and external circuit for a typical heating and cooling day (17/02/2010 — 20/09/2010).

341 sealed with bentonite on the top. Further details about the ground heat
342 exchanger can be found in [47].

343 There are two temperature sensors located at the entrance and the exit
344 of each borehole, measuring the water temperature at those points. Fur-
345 thermore, there are several temperature sensors in 3 of the 6 boreholes,
346 which are located at different depths between the upward and downward
347 pipes.

348 Ground thermal properties were determined by means of laboratory
349 analysis, using dry soil samples. For the thermal conductivity, a value
350 of 1.43 W/mK was obtained, although a high uncertainty (around 20%)
351 was observed. A value of 2.25MJ/m³K was obtained for the volumetric
352 heat capacity. However, the groundwater level is about 3.5 m. So, the
353 effective values of the ground thermal conductivity and capacity could be
354 significantly higher.

355 *3.2. TRNSYS simulation*

356 This section presents the validation of B2G against experimental mea-
357 surements of one of the six boreholes of the GeoCool plant [8]. For this
358 purpose, B2G has been implemented in the TRNSYS software, creating
359 a new TRNSYS type. The experimental measurements of mass flow rate
360 and of inlet water temperature have been used as inputs for the model at
361 each simulation time step (1 minute). Finally, the calculated outlet fluid
362 temperature at the U-tube has been compared against the experimental
363 measurements.

364 The model has been validated considering two different operating con-
365 ditions: a step-test in cooling mode (performed on 04/11/2013) and the

366 standard operating condition in two different typical days, one for heating
367 mode (15/02/2010) and one for cooling mode (15/09/2010). The following
368 assumptions have been made:

- 369 • The thermophysical properties of the ground and the grout have been
370 increased considering that, as already stated in section 3.1.1, the
371 groundwater level is about 3.5 m and the effective values of the conduc-
372 tivity and the volumetric thermal capacitance could vary significantly.
- 373 • The equivalent diameter has been calculated using the approximation
374 suggested by Pasquier et al. [30] (see section 2.1, Eq. 12).
- 375 • The studied borehole is provided with spacers that ensure a value of
376 70 mm for the shank spacing. However, considering that the U-tube
377 is not fixed inside the borehole and, therefore, the centering is not
378 guaranteed, the borehole nodes have been located on the borehole
379 wall, as suggested by Lamarche et al. [31] for pipe positions close to
380 the borehole wall.
- 381 • The thermal capacitance of the ground node, C_g , has been deducted
382 in order to obtain a good correspondence at the end of the 24 hours of
383 simulation, since this is the time interval that the model is intended
384 to reproduce.

385 Table 1 shows the values of all the parameters of the TRNSYS type
386 considered in the present work. These parameters correspond to the ones
387 required by the B2G model (note that thermal capacitances and resistances
388 are node values and, in this form, they depend on the number of nodes
389 adopted).

Thermophysical properties		
Ground thermal conductivity	k_g	2.09 $Wm^{-1}K^{-1}$
Grout thermal conductivity	k_b	2.09 $Wm^{-1}K^{-1}$
Ground volumetric thermal capacitance	c_g	3200 $kJm^{-3}K^{-1}$
Grout volumetric thermal capacitance	c_b	3200 $kJm^{-3}K^{-1}$
Ground thermal diffusivity	α_g	0.002351 m^2h^{-1}
Geometrical characteristics		
Borehole diameter	D_b	150 mm
External U-pipe diameter	$D_{p,e}$	32 mm
Internal U-pipe diameter	$D_{p,i}$	25.4 mm
Shank spacing (center-to-center)	W	70 mm
Depth	L	50 m
Model parameters		
Number of nodes	n	150 -
Borehole node thermal capacitance	$C_{b1} - C_{b2}$	17.56 JK^{-1}
Ground node thermal capacitance	C_g	1200 JK^{-1}
Borehole conductive thermal resistance	$R_{b1} - R_{b2}$	0.2738 KW^{-1}
Pipe to pipe thermal resistance	R_{pp}	0.8525 KW^{-1}
Borehole to borehole thermal resistance	R_{bb}	0.4257 KW^{-1}
Borehole to ground thermal resistance	R_g	0.2772 KW^{-1}
Equivalent pipes diameter	D_{eq}	45 mm
Borehole node position	D_x	150 mm
Ground radial penetration diameter	D	860 mm
Ground nodes position	D_1	505 mm

Table 1: Main parameter adopted in the present work.

390 4. Results and discussion

391 4.1. Step-test

392 Since the GeoCool plant performance is based on on/off cycles, adjusting
393 and validating the model parameters with experimental data of a typical day
394 becomes a difficult task. In order to obtain a suitable set of experimental
395 data, a step-test was performed in the installation, on November 2013.

396 The test was carried out with the heat pump configured in cooling mode
397 (condenser heat injected into the ground source heat exchanger). The main
398 objective of the test was to obtain experimental data for a period of a few
399 hours, with the heat pump continuously running in all the period, and with
400 a thermal load approximately constant. For this purpose, the thermal load
401 of the building was increased by means of electric heaters which were located
402 in the air-conditioned offices, in order to increase the thermal demand of the
403 building and avoid the cycling of the heat pump during the step test. Figure
404 8 shows the evolution of the water temperatures entering and exiting the
405 ground loop during the test. The water temperatures presented in Figure 8
406 correspond to the inlet and outlet temperatures of the internal and external
407 circuit, measured at the heat pump (T_{inIC} , T_{outIC} , T_{inEC} , T_{outEC}). The
408 internal and external circuit mass flow rates are also presented in Figure 8.
409 Looking at the evolution of the water flow rate at the internal and external
410 circuit, it is possible to know how the test was carried out.

- 411 • At 7:00 h the internal circulation pump was switched on, according
412 to the schedule of the installation.
- 413 • At 10:00 h the test started, switching on the external circulation
414 pump, but not the heat pump, and letting the water circulate without

415 any thermal load being injected, so as to know the initial conditions
416 for the water and the ground temperature. During this period of time,
417 the internal circuit water temperatures increase, since the heat pump
418 is switched off while the fancoils and the internal circulation pump
419 are switched on.

- 420 • At 13:50 h the heat pump was switched on.
- 421 • At 20:55 h the internal circulation pump and the heat pump were
422 switched off, according to the installation schedule. However, the
423 external circulation pump was forced to remain switched on in order
424 to produce a recovery step until 9:00 h of the next day, which was also
425 useful for the model validation.

426 For model validation purposes, only the test period data are used, i.e.
427 starting from 9:00 and for a total of 24 hours. The water temperature at
428 the inlet of the borehole is used as input to the model. The simulated outlet
429 water temperature is compared with the experimental one. Since equalizing
430 valves have been installed in the BHE, the total mass flow rate is equally
431 distributed between the six boreholes, thus the simulation flow rate for the
432 model can be obtained dividing the total mass flow rate, experimentally
433 measured, by six. Finally, using the parameters of Table 1, the simulation
434 results of the model are shown in Figure 9.

435 As shown in Figure 9a, B2G correctly reproduces the evolution of the
436 water temperature at the outlet of the borehole. The simulation results
437 present a good agreement with the experimental ones with only a little de-
438 viation at around one hour after the starting of the test, reflecting that
439 real results present a slightly higher inertia than the ones predicted by the

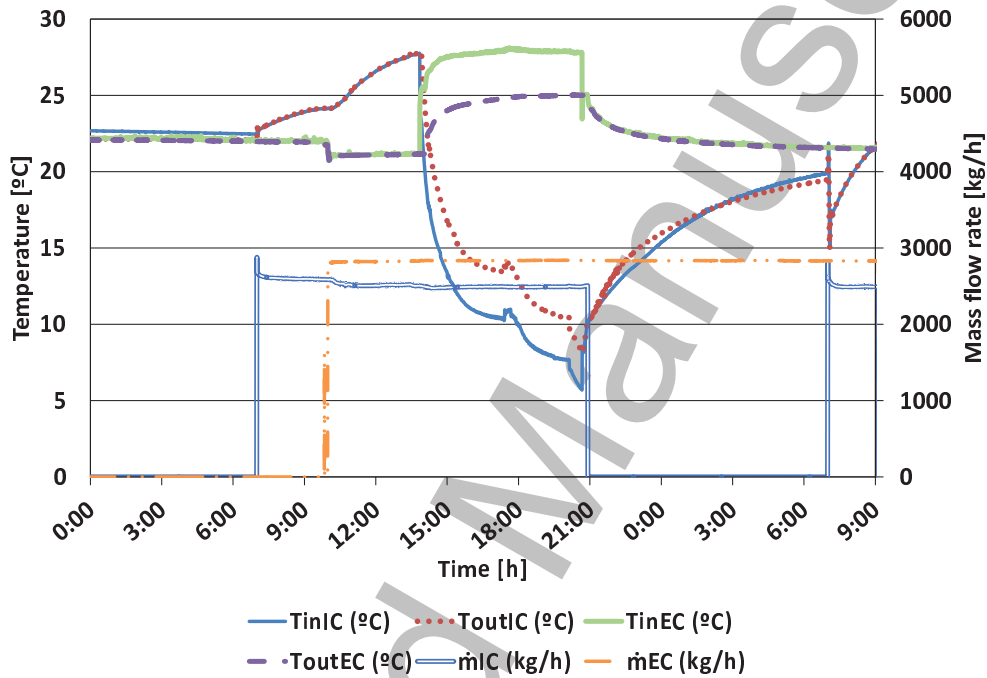


Figure 8: Step-test: water temperatures and flow rates at both sides of the heat pump. T_{inIC} : internal circuit inlet temperature. T_{outIC} : internal circuit outlet temperature. T_{inEC} : external circuit inlet temperature. T_{outEC} : external circuit outlet temperature.

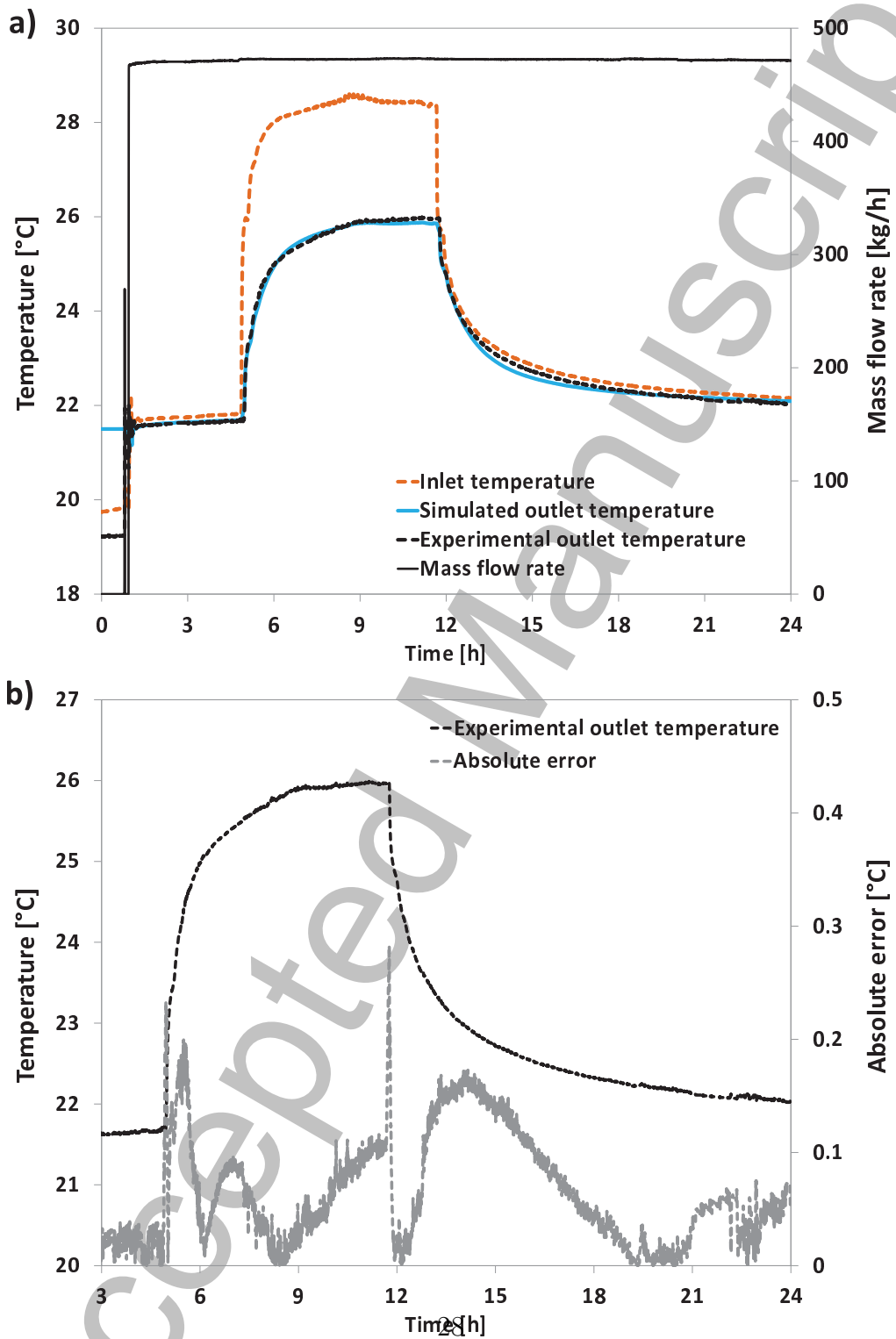


Figure 9: Step-test simulation result. a) Temperature and mass flow rate profiles. b) Absolute error between simulated and experimental outlet water temperature profiles.

440 model. The same deviation can be observed in the recovery step. However,
441 the medium-term results tend to the experimental data, even after 24 hours
442 of simulation. Moreover, Figure 9b reports the correspondent absolute er-
443 ror between experimental and numerical results, showing that B2G is able
444 to reproduce the outlet temperature profile with a maximum error of 0.3
445 K in correspondence of the injection pulse, where the dynamic effects are
446 stronger. Therefore, it can be concluded that B2G is able to reproduce the
447 outlet water temperature evolution in the short-term with a high accuracy.

448 4.1.1. D_x analysis

449 The previous results were obtained by assuming the borehole nodes to be
450 located at the borehole wall ($D_x = D_b$). This assumption must be checked
451 with a sensitivity analysis of the position of the borehole nodes. The value
452 of D_x is calculated as shown in Eq. 20, considering that the borehole nodes
453 have to be located somewhere in between D_{eq} and D_b .

$$D_x = a(D_b) + (1 - a)D_{eq} \quad \text{with } 0 < a < 1 \quad (20)$$

454 Figure 10 shows the comparison between the simulated outlet water tem-
455 perature and the experimental one, for different values of D_x , corresponding
456 to different values of the parameter a ($a = [1, 0.9, 0.8, 0.7, 0.6, 0.5]$). As it
457 can be observed in Figure 10a, differences between simulation results are
458 negligible after a few hours. Differences in the short-term response are high-
459 lighted in Figure 10b which shows an amplified view of the first hours of
460 the step.

461 Results show that situating the nodes at the borehole wall produces the
462 best fitting. Therefore, the initial assumption made in this work is validated,
463 also verifying the suggestion made by Lamarche et al. [31].

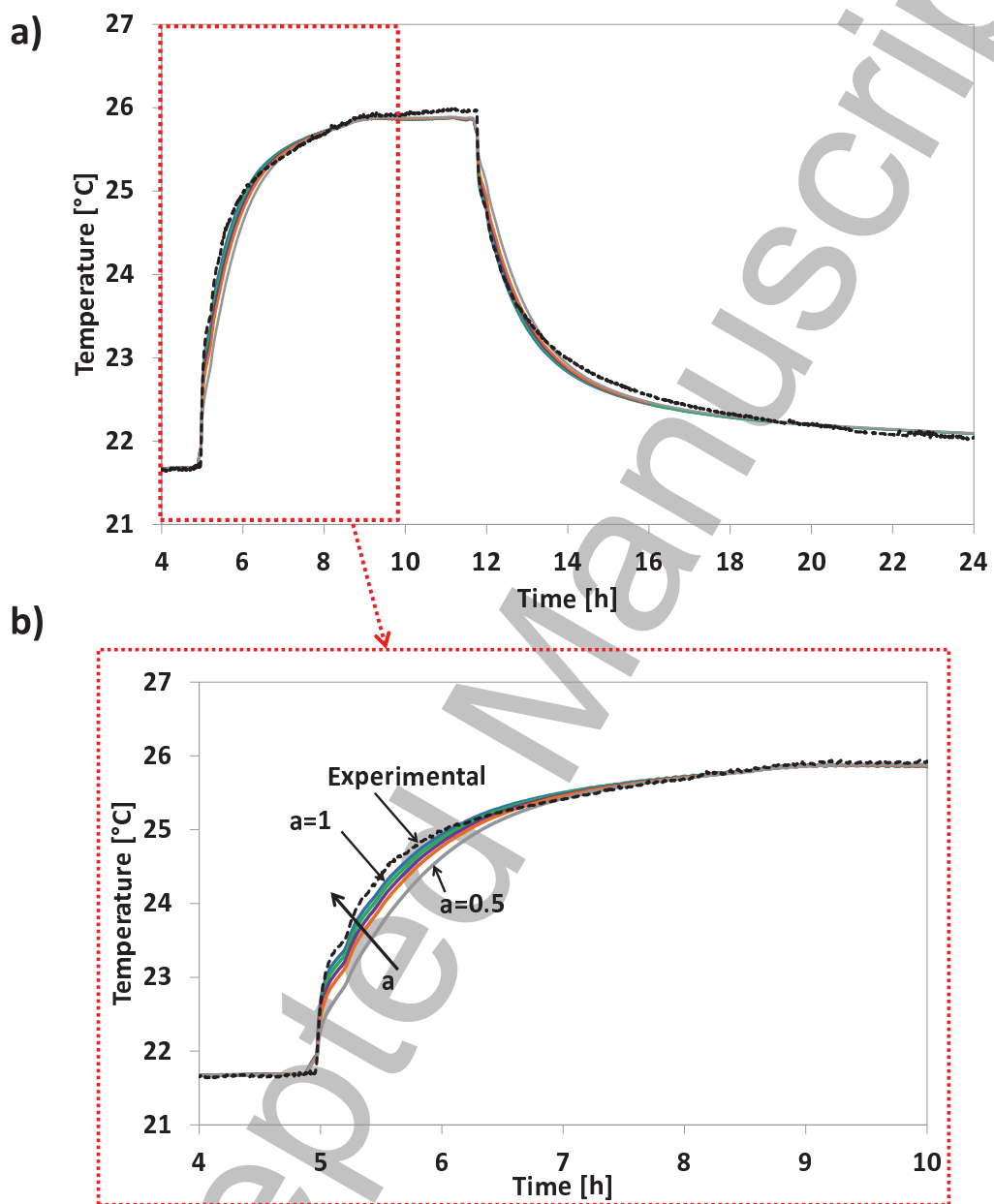


Figure 10: Step-test: sensitivity analysis of the position of the borehole nodes.

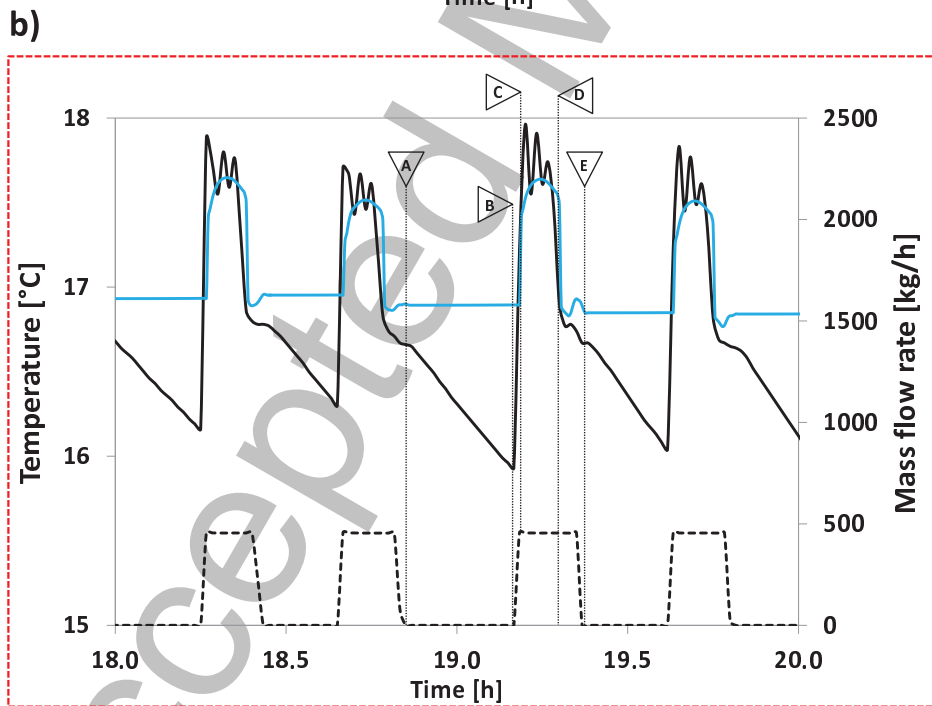
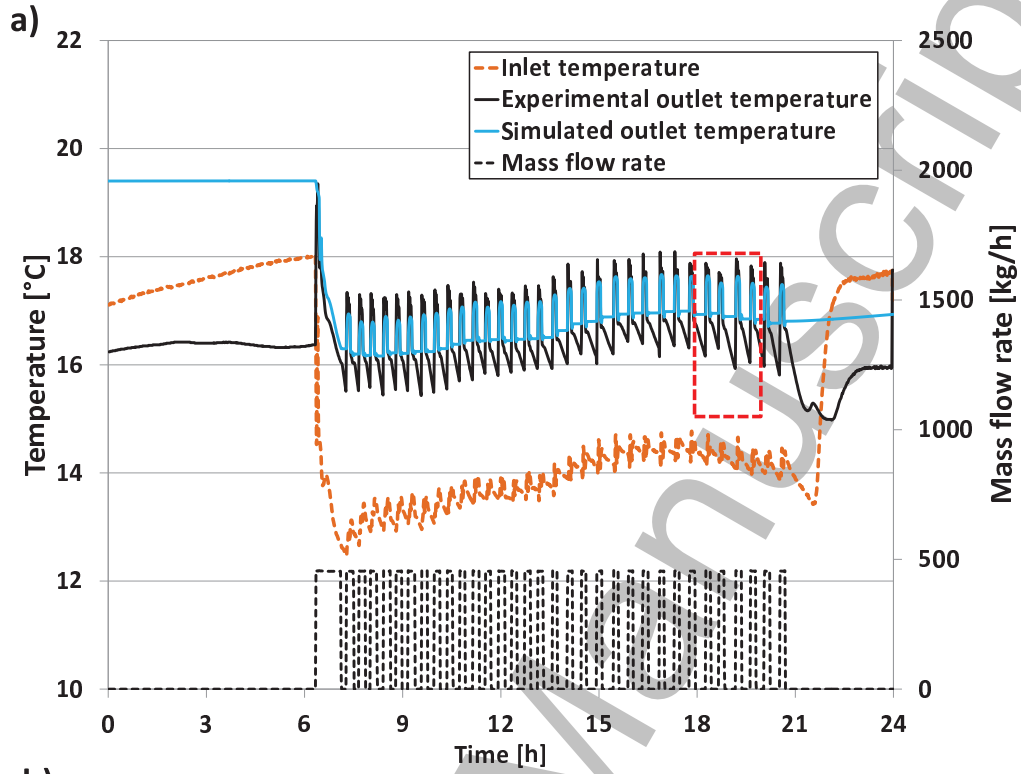
464 *4.2. Typical day performance*

465 The model will be now double-validated against experimental data cor-
466 responding to the typical daily operation of GeoCool plant. The water
467 temperature profiles for typical heating and cooling days have been pre-
468 sented in Figure 7. The water temperatures from the same borehole is used
469 for simulation and validation of B2G model. The results of the simulations
470 for both heating and cooling days are shown in Figures 11 and 12, compared
471 with the experimental results.

472 As in the previous section, the borehole inlet water temperature is em-
473 ployed as the input for the B2G model, and the calculated outlet temper-
474 ature is then compared with the experimental measurements. The initial
475 temperature for the borehole model has been determined taking into ac-
476 count the first peak in the outlet temperature, that corresponds to the
477 water inside the borehole during the night.

478 Figure 11b shows an augmented section of the borehole outlet water
479 temperature shown in Figure 11a, for heating mode, where the short-term
480 response of the model can be analyzed. In order to better understand the
481 simulation results, critical points (A-E) have been identified in Figure 11b.

482 During the OFF cycle, i.e. from A to B points of Figure 11b (see that
483 the mass flow rate, also shown in Figure 11, is null during this period), the
484 experimental temperature measured at the outlet of the borehole tends to
485 the ambient temperature, which in winter means that it decreases during
486 this period. Actually, since there is no water flow rate as the external
487 circulation pump is switched off during these intervals, this behavior does
488 not reflect the borehole thermal performance but it is more related with
489 the ambient temperature, which has a greater influence on the top of the



32

Figure 11: Typical heating day simulation results (15/02/2010).

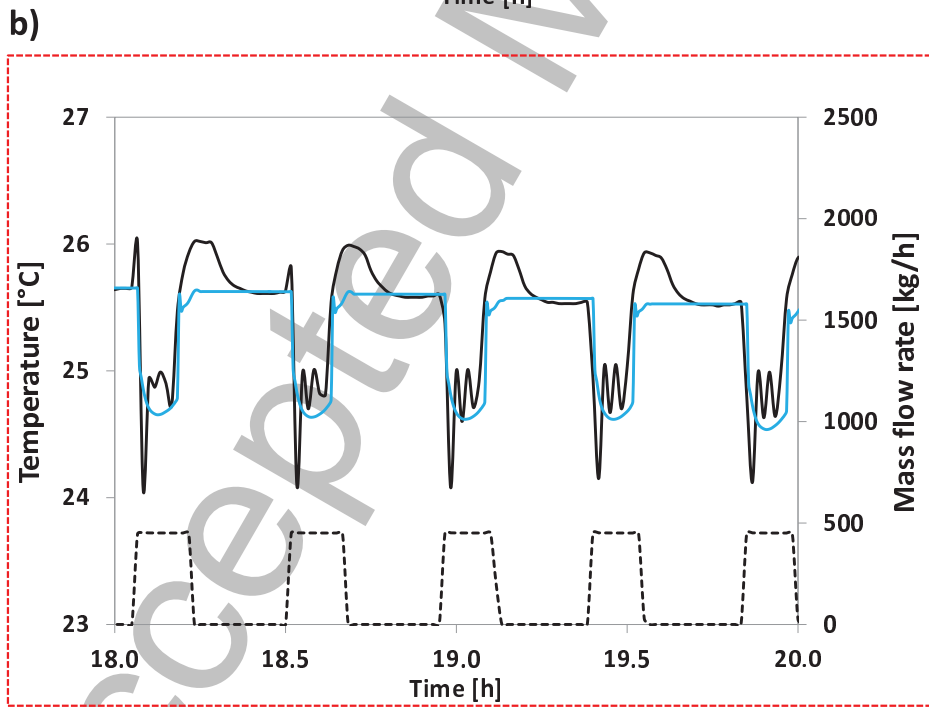
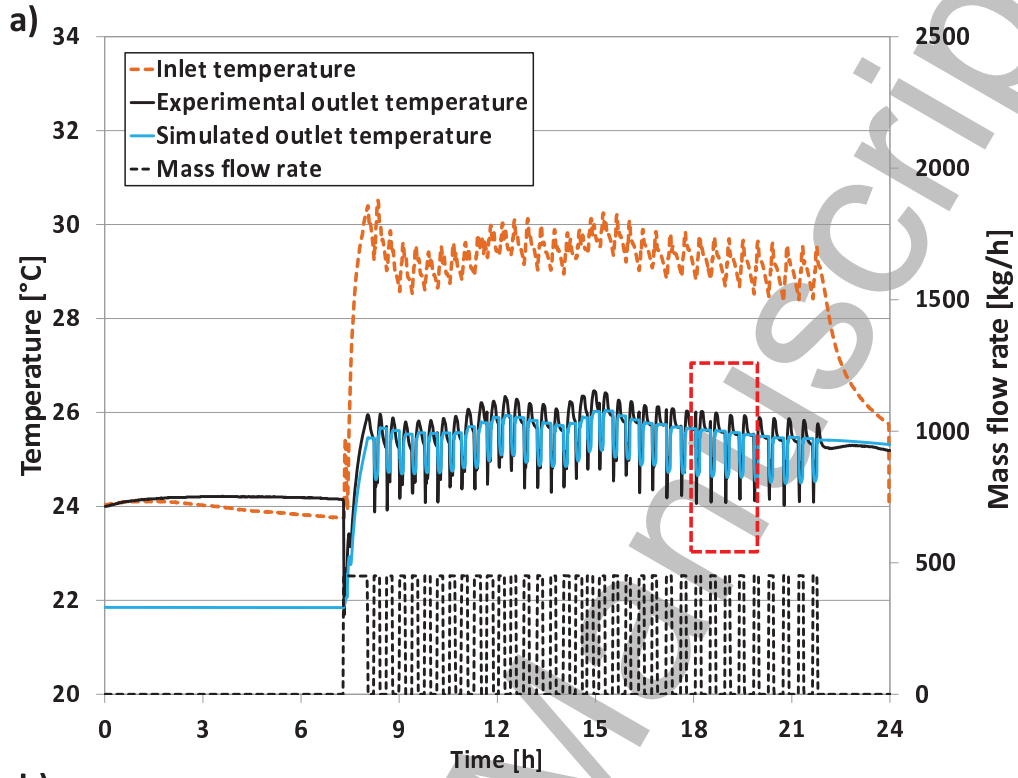


Figure 12: Typical cooling day simulation results (15/09/2010).

490 borehole, closer to the surface. However, the simulated temperature remains
491 nearly constant during the OFF periods. This is due to the fact that the
492 influence of the ambient temperature on the upper borehole nodes has not
493 been taken into account, as it is out of the scope of the proposed model, since
494 it happens out of the borehole. Besides, once the circulation pump switches
495 on again (point B) and the water starts moving, the experimental water
496 temperature suddenly increases (point C), reaching the same values than
497 the simulated one. It can be concluded, then, that the observed differences
498 in the temperature evolution of the last borehole node during the OFF
499 periods (between points A and B) have no influence in the temperature
500 evolution once the circulation pump is switched on, so, they must not be
501 considered in the comparison.

502 At the start of the ON periods, from B to C points, the temperature
503 suddenly increases. This is due to the displacement of the water that re-
504 mains inside the borehole during the OFF period, whose temperature tends
505 to the ground temperature. The water that enters in the borehole at the
506 start of the ON period (point C) takes some time (about 7 minutes) to
507 travel through the U-tube, corresponding to the duration of the temper-
508 ature peak, that is, from point C to D of Figure 11b. Once this water
509 reaches the end of the borehole, a temperature decrease can be observed at
510 the outlet temperature curve (point D). The predicted outlet temperature
511 perfectly reproduces all these phenomena, achieving the main objective of
512 the model: to correctly reproduce the short-term behavior of the borehole
513 heat transfer and, therefore, of the outlet water temperature. The differ-
514 ences found in the shape of the experimental and simulated curves can be
515 attributed to the temperature measurement uncertainty, and the vertical

516 heat transfer effects which are neglected in the B2G model.

517 Taking a more general look at the temperature evolution during the day,
518 it can be checked that the behavior observed in the step-test validation is
519 reflected in this simulation. As expected, B2G simulation results for the
520 water temperature evolution accurately reproduce the experimental ones,
521 with almost negligible deviations after the first hour that reflect a slightly
522 lower thermal inertia in the simulated results than in reality. At the end of
523 the operating time, though, this difference is negligible.

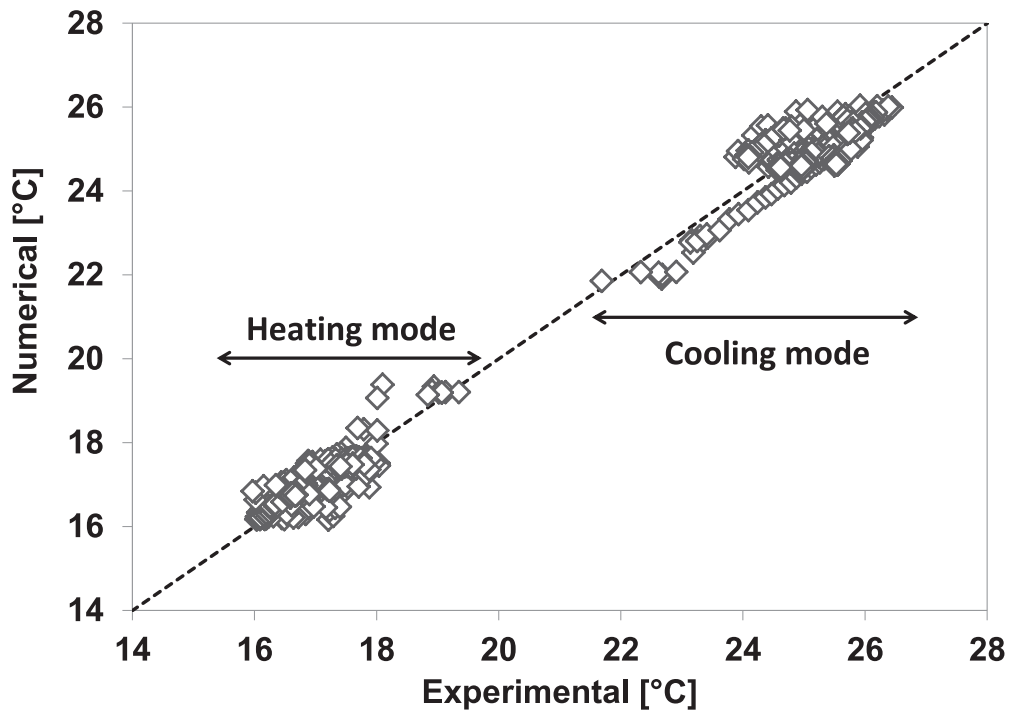


Figure 13: Experimental VS numerical outlet water temperature values for both heating and cooling cases.

524 The B2G response for cooling mode (Figure 12) presents the same evo-

525 lution. Even if the temperature values are not so exactly adjusted, it can be
526 considered that the B2G behavior still represents the reality with enough
527 accuracy, double-validating the proposed model.

528 Finally, Figure 13 reports the comparison between predicted and exper-
529 imental outlet water temperature values for both heating and cooling cases.
530 As it is possible to observe, B2G is able to reproduce correctly the outlet
531 water temperature despite the strong dynamic effects which occur during
532 ON-OFF operating conditions.

533 **5. Conclusions**

534 Decoupling short-term and long-term responses allows the use of faster
535 BHE models in both time scales, which can be combined lately to form a
536 global model.

537 In this context, the B2G model is based on a thermal network approach,
538 coupled with a vertical discretization of the borehole, focused on modelling
539 the short-term response of a BHE. Several calculation techniques have been
540 proposed in order to calculate the model parameters.

541 B2G was validated against experimental data from GeoCool plant, at
542 Universitat Politècnica de València, Spain. Most of the parameters of the
543 model could be estimated from a theoretical approach. The ones that re-
544 mained as adjusting parameters have been adjusted using experimental data
545 from a step-test performed at the installation without any other facility or
546 machinery than the one already present at the system. So, the model can be
547 easily adjusted to any installation by conducting a simple step-test similar
548 to the one described in this work.

549 The final validation of B2G was performed considering standard oper-
550 ating conditions for two different days in heating and cooling mode. The
551 results highlight that B2G is able to reproduce the outlet water temperature
552 profiles for all tested operating conditions, showing a good agreement with
553 the experimental measurements.

554 **6. Acknowledgements**

555 The present work has been supported by the FP7 European project
556 Advanced ground source heat pump systems for heating and cooling in
557 Mediterranean climate (GROUND-MED).

Nomenclature	
α	Thermal diffusivity [m^2/s]
BHE	Borehole heat exchanger
c	Volumetric thermal capacity [$\text{J}/\text{m}^3\text{K}$]
C	Thermal capacitance [J/K]
D	diameter [m]
GSHE	Ground source heat exchanger
GSHP	Ground source heat pump
k	conductivity [W/mK]
h	convective heat transfer coefficient [$\text{W}/\text{m}^2\text{K}$]
L	depth [m]
\dot{m}	Mass flow rate [kg/h]
n	number of nodes [-]
Nu	Nusselt number [-]
r	radius [m]
R	Thermal resistance [K/W]
R_{BHE}	Borehole thermal resistance [mK/W]
R_{12}	Fluid to fluid thermal resistance [mK/W]
S	surface [m^2]
t	Time [s]
T	Temperature [$^{\circ}\text{C}$]
v	velocity [m/s]
W	shank spacing [m]
z	Borehole depth coordinate [m]
Subscripts	
1	Downward pipe zone
2	Upward pipe zone
b	borehole
bb	borehole node to borehole node
c	conduction
e	external
EC	External circuit (ground loop)
eq	equivalent
g	ground
gp	ground penetration
j	j-node
h	convection
i	internal
IC	Internal circuit (building)
in	Inlet
p	pipe
pp	pipe node to pipe node
out	Outlet
x	borehole node position

560 References

- 561 [1] Environmental Protection Agency:
562 http://www.epa.gov/region1/eco/energy/re_geothermal.html, 14/03/2013.
- 563 [2] Hepbasli A, Akdemir O, Hancioglu E. Experimental study of a closed loop vertical
564 ground source heat pump system. *Energ Convers Manage* 2003;44:527-48.
- 565 [3] Li M, Lai ACK. Thermodynamic optimization of ground heat exchangers with sin-
566 gle U-tube by entropy generation minimization method. *Energ Convers Manage*
567 2013;65:133-9.
- 568 [4] Kizilkan O, Dincer I. Borehole thermal energy storage system for heating applica-
569 tions: Thermodynamic performance assessment. *Energ Convers Manage* 2015;90:53-
570 61.
- 571 [5] Kurevija T, Vulin D, Krapec V. Effect of borehole array geometry and thermal
572 interferences on geothermal heat pump system. *Energ Convers Manage* 2012;60:134-
573 42.
- 574 [6] Zhang C, Chen P, Liu Y, Sun S, Peng D. An improved evaluation method for thermal
575 performance of borehole heat exchanger. *Renew Energ* 2015;77:142-51.
- 576 [7] Shirazi AS, Bernier M. Thermal capacity effects in borehole ground heat exchangers.
577 *Energ Buil* 2013;67:352-64.
- 578 [8] Ruiz-Calvo F, Montagud C. Reference data sets for validating GSHP system mod-
579 els and analyzing performance parameters based on a five-year operation period.
580 *Geothermics* 2014;51:417-428.
- 581 [9] Wu W, You T, Wang B, Shi W, Li X. Evaluation of ground source absorption heat
582 pumps combined with borehole free cooling. *Energ Convers Manage* 2014;79:334-43.
- 583 [10] Yoon S, Lee SR, Go GH. A numerical and experimental approach to the estimation
584 of borehole thermal resistance in ground heat exchangers. *Energy* 2014;71:547-55.
- 585 [11] Ruiz-Calvo F, De Rosa M, Acuña J, Corberán JM, Montagud C. Experimental
586 validation of a short-term Borehole-to-Ground (B2G) dynamic model. *Appl Energ*
587 2015;140:210-23.
- 588 [12] Monzó P, Mogensen P, Acuña J, Ruiz-Calvo F, Montagud C. A novel numerical
589 approach for imposing a temperature boundary condition at the borehole wall in
590 borehole fields. *Geothermics* 2015;56:35-44.

- 591 [13] Self SJ, Reddy BV, Rosen MA. Geothermal heat pump systems: Status review and
592 comparison with other heating options. *Appl Energ* 2013;101:341-8.
- 593 [14] Yang H, Cui P, Fang Z. Vertical-borehole ground-coupled heat pumps: A review of
594 models and systems. *Appl Energ* 2010;87:16-27.
- 595 [15] Eskilson P. Thermal analysis of heat extraction boreholes. PhD Thesis, University
596 of Lund, Sweden; 1987.
- 597 [16] Michopoulos A, Kyriakis N. Predicting the fluid temperature at the exit of the
598 vertical ground heat exchangers. *Appl Energ* 2009;86:2065-70
- 599 [17] Yavuzturk C, Spitler JD. A Short Time Step Response Factor Model for Vertical
600 Ground Loop Heat Exchangers. *ASHRAE Trans* 1999;105(2):475-85.
- 601 [18] Spitler JD. GLHEPRO – A Design Tool For Commercial Building Ground Loop Heat
602 Exchangers. Proceedings of the Fourth International Heat Pumps in Cold Climates
603 Conference, Aylmer, Qubec. August 17-18; 2000.
- 604 [19] Hellström G, Sanner B. Earth energy designer: software for dimensioning of deep
605 boreholes for heat extraction. Sweden: Department of Mathematical Physics, Lund
606 University; 1994.
- 607 [20] Acuña J, Fossa M, Monzó P, Palm B. Numerically Generated g-functions for Ground
608 Coupled Heat Pump Applications. Proceedings of the 2012 COMSOL Conference;
609 2012.
- 610 [21] Deerman JD, Kavanaugh SP. Simulation of vertical U-tube ground coupled
611 heat pump systems using the cylindrical heat source solution. *ASHRAE Trans*
612 1991;97:287-95.
- 613 [22] Kavanaugh SP, Rafferty K. Ground-Source Heat Pumps Design of Geothermal
614 System for Commercial and Institutional Buildings. ASHRAE, Atlanta, 1997.
- 615 [23] ASHRAE Handbook-HVAC Applications, Geothermal Energy. 2003 (Chapter 32).
- 616 [24] Fossa M. The temperature penalty approach to the design of borehole heat exchang-
617 ers for heat pump applications. *Energ Build* 2011;43:1473-9.
- 618 [25] Koochi-Fayegh S, Rosen MA. An analytical approach to evaluating the effect of
619 thermal interaction of geothermal heat exchangers on ground heat pump efficiency.
620 *Energ Convers Manage* 2014;78:184-92.
- 621 [26] Zarrella A, Scarpa M, De Carli M Short time-step analysis of vertical ground-coupled

- 622 heat exchangers: The approach of CaRM. *Renew Energ* 2011;36:2357-67.
- 623 [27] Eskilson P, Claesson J. Simulation model for thermally interacting heat extraction
624 boreholes. *Num Heat Transf* 1988;13:149-65.
- 625 [28] Bauer D, Heidemann W, Müller-Steinhagen H, Diersch HJG. Thermal resistance
626 and capacity models for borehole heat exchangers. *Int J Energ Res* 2011;35:31220.
- 627 [29] Bauer D, Heidemann W, Diersch HJG. Transient 3D analysis of borehole heat ex-
628 changer modeling. *Geothermics* 2011;40:250-60.
- 629 [30] Pasquier P, Marcotte D. Short-term simulation of ground heat exchanger with an
630 improved TRCM. *Renew Energ* 2012;46:92-9.
- 631 [31] Lamarche L, Kajl S, Beauchamp B. A review of methods to evaluate borehole ther-
632 mal resistances in geothermal heat-pump systems. *Geothermics* 2010;39:187-200.
- 633 [32] Sharqawy MH, Mokheimer EM, Badr HM. Effective pipe-to-borehole thermal resis-
634 tance for vertical ground heat exchangers. *Geothermics* 2009;38:271-77.
- 635 [33] Diersch HJG, Bauer D, Heidemann W, Rühaak W, Schätzl P. Finite element mod-
636 eling of borehole heat exchanger systems Part 1: Fundamentals. *Computers & Geo-
637 sciences* 2011;37:1122-35.
- 638 [34] Diersch HJG, Bauer D, Heidemann W, Rühaak W, Schätzl P. Finite element mod-
639 eling of borehole heat exchanger systems Part 2. Numerical simulation. *Computers
640 & Geosciences* 2011;37:1136-47.
- 641 [35] Esen H, Inalli M, Esen Y. Temperature distributions in boreholes of a vertical
642 ground-coupled heat pump system. *Renew Energ* 2009;34:2672-9.
- 643 [36] Lee CK, Lam HN. Computer simulation of borehole ground heat exchangers for
644 geothermal heat pump systems. *Renew Energ* 2008;33:1286-96.
- 645 [37] Zarrella A, Scarpa M, De Carli M. Short time-step performances of coaxial and
646 double U-tube borehole heat exchangers: Modeling and measurements. *HVAC&R
647 Research* 2011;17(6):959-76.
- 648 [38] Yang W, Shi M, Liu G, Chen Z. A two-region simulation model of vertical U-tube
649 ground heat exchanger and its experimental verification. *Appl Energ* 2009;86:2005-
650 12.
- 651 [39] Oppelt T, Riehl I, Gross U. Modelling of the borehole filling of double U-pipe heat
652 exchangers. *Geothermics* 2010;39:270-6.

- 653 [40] Esen H, Inalli M. Modelling of a vertical ground coupled heat pump system by using
654 artificial neural networks. *Expert Systems with Applications* 2009;36:10229-38.
- 655 [41] Montagud C, Corberán JM, Ruiz-Calvo F. Experimental and modeling analysis of
656 a ground source heat pump system. *Appl Energ* 2013;109:328-36.
- 657 [42] University of Wisconsin-Madison. A TRaNsient SYtems Simulation program.
658 <http://sel.me.wisc.edu/trnsys/> [accessed 24/02/2014].
- 659 [43] De Rosa M, Ruiz-Calvo F, Corberán JM, Montagud C, Tagliafico LA. Borehole
660 modelling: a comparison between a steady-state model and a novel dynamic
661 model in a real ON/OFF GSHP operation. *Journal of Physics: Conference Series*
662 2014;547:012008.
- 663 [44] Hellström G. Duct Ground Heat Storage. Manual for Computer Code. 1989. De-
664 partment of Mathematical Physics, University of Lund.
- 665 [45] GeoCool project (EU 5th Framework Programme, NNE5-2001-00847),
666 http://cordis.europa.eu/projects/rcn/86940_en.html
- 667 [46] Gnielinsky V. New equations for heat and mass transfer in turbulent pipe and
668 channel flow. *International Chemical Engineering* 1976;16:359-68.
- 669 [47] Magraner T. Validación Experimental de los Métodos de Diseño de Instalaciones de
670 Bomba de Calor Acoplada al Terreno. PhD thesis, UPVLC; 2010.
- 671 [48] Montagud C, Corberán JM, Montero Á, Urchueguía JF. Analysis of the energy
672 performance of a Ground Source Heat Pump system after five years of operation.
673 *Energ Buildings* 2011;43:3618-26.